*Article*

# A Pixel-Scale Measurement Method of Soil Moisture Using Ground-Penetrating Radar

**Wenlong Song [1,2], Yizhu Lu [1,2,\*], Yu Wang [3], Jingxuan Lu [1,2] and Haixian Shi [3]**

1    Sate Key Laboratory of Simulation and Regulation of Water Cycle in River Basin, China Institute of Water Resources and Hydropower Research, Beijing 100038, China; songwl@iwhr.com (W.S.)
2    Research Center on Flood & Drought Disaster Reduction of the Ministry of Water Resources, China Institute of Water Resources and Hydropower Research, Beijing 100038, China
3    City River and Lake Management Office of Beijing, Beijing 100089, China
\*    Correspondence: luyzh@iwhr.com; Tel.: +86-010-6878-5451

**Abstract:** Ground validation of remote sensing soil moisture requires ground measurements corresponding to the pixel scale. To date, there is still a lack of simple, fast and reasonable methods for soil moisture measurement at pixel scale between point measurements and remote sensing observations. In this study, a measurement method of soil moisture using ground-penetrating radar (GPR) was proposed for pixel scale. We used a PulseEKKOTM PRO GPR system with 250 MHz antennas to measure soil moisture by Fixed Offset (FO) method in four $30 \times 30$ m$^2$ plots chosen from the desert steppe. This study used a random combination method to analyze soil moisture measurements acquired by different numbers of GPR survey lines. The results showed that two survey lines of GPR would be sufficient under confidence level of 90% with the relative error of 7%, and four survey lines of GPR would be eligible under confidence level of 95% with the relative error of 5% for each plot. GPR measurement can reproduce the spatial distribution of soil moisture with higher resolution and smaller error, especially when two and four survey lines are designed in cross shape and grid shape, respectively. The method was applied to ground validation for the soil moisture from Landsat 8, showing the advantages of stable relative errors, less contingency and reliable evaluation when compared to point measurements. This method is fast and convenient and not limited to a certain pixel, and thus largely benefits the scale matching of remote sensing results and field measurements in ground validation.

**Keywords:** ground-penetrating radar; soil moisture; remote sensing pixel; scale issue; ground validation

## 1. Introduction

Soil moisture plays an effective role in the hydrological cycle because of its relationship with precipitation, evapotranspiration (ET), irrigation practice and crop growth [1,2]. Low soil moisture affects the growth and health of crops through poor nutrient absorption, soil erosion and the proliferation of pests, especially during the key growth stages of crops, resulting in agricultural drought and even yield reduction [3–5]. Additionally, spatial and temporal soil moisture dynamics are important for crop yield forecasting, early warning of droughts, identification and assessment of drought, managing insect and disease control, and planning irrigation scheduling [6–9].

Satellite remote sensing provides a unique opportunity for large-scale soil moisture measurement, even in a near real-time manner [10,11]. In China, high-resolution satellite-based soil moisture products are generally utilized to identify and assess agricultural drought across large areas. Landsat series and Huan Jing-1 satellite images are the most commonly used data sources of remote sensing in China, with a resolution of 30 m. The reliability of remote sensing results is generally validated with the field measurement data corresponding to image pixels, for example, using point-scale measurements by the gravimetric method, TDR or neutron probe. The gravimetric method is the most commonly

used method of obtaining point measurements to evaluate remote sensing data [12,13], but it has the disadvantages of being time-consuming, labor-intensive and damaging to soil structure. Therefore, there is a scale mismatch problem when using typical point measurements to evaluate pixel-scale soil moisture measurements by remote sensing. Thus, many sampling methods were developed to estimate the necessary sampling size of point measurements for a rational mean value at pixel scale, such as statistical sampling, geostatistical sampling, stratified sampling, the bootstrap method and random combination method [14–18]. However, these methods require a large number of point measurements as a basis to analyze the necessary sampling size, which need to be recalculated for other pixels and other times. Therefore, there is a lack of reasonable and fast methods between fixed-point measurements and remote sensing data to measure pixel-scale soil moisture that can reduce errors of evaluation caused by scale issue.

Since Huisman et al. presented the basic theoretical principles of soil moisture measurements by GPR, research and application of GPR have been increasing rapidly within the last two decades [19,20]. New methods of GPR data acquisition and analysis are constantly being improved [21]. GPR is highly sensitive to changes in soil moisture and is widely used at field scale [22]. A series of research has proved the ability of GPR to measure soil moisture with the advantages of high accuracy, flexible maneuverability, higher spatial resolution, fast measurement and a deeper investigation extent [12,19,20,23,24]. The measuring accuracy of GPR has been verified by measurements using the gravimetric method, TDR, lysimeter and the neutron method [19,25,26]. monitored soil moisture dynamics by GPR and further compared measurements with simulated soil moisture profiles by unsaturated flow model, achieving very good agreement [27]. Liu et al. proposed a new method of quantifying root zone soil moisture by GPR, and extended the application of GPR to the root zone [28]. As a nondestructive geophysical method, the fixed offset (FO) method of GPR has the ability to monitor soil moisture by survey lines and quantify the spatial variation of soil moisture, bridging the scale gap between remote sensing and accurate point measurements [29–31]. It can play an active role in the ground validation of soil moisture by remote sensing, and provides the possibility of scale matching remote sensing results and field measurements. To date, GPR technology has still not been applied to evaluate remote sensing results. In this study, we have made attempts to validate remote sensing soil moisture with GPR, with a focus on the key question of how many survey lines of GPR are necessary, and how to layout survey lines in pixels for estimating a rational mean value under a given relative error. We aim to propose a pixel-scale measurement method of soil moisture based on GPR. The measurement experiment of soil moisture at multi-scale was carried out in a steppe desert of Inner Mongolia, in which the type of land use and land cover is uniform, and the measuring accuracy of soil moisture by GPR had been inspected by gravimetric data in a previous study [32]. This study applied a random combination method to analyze soil moisture measurements of a pixel by different numbers of GPR survey lines within different relative errors, and compared different layouts of survey lines by universal kriging interpolation. Then, the applicability of this pixel-scale measurement method using GPR was tested for a pixel with a resolution of 60 m. Finally, the pixel-scale measurement method of GPR and the sampling method of point measurements were compared in the ground validation of remote sensing soil moisture from Landsat 8.

## 2. Study Area

This experiment was conducted at the experimental base of the Institute of Water Resources for Pastoral in Xilamuren Town, Baotou City, of the Inner Mongolia region (41°22′ N, 111°12′ E) (Figure 1). The experimental base, located in the Wulanchabu desert steppe of the central Inner Mongolia Region, adjacent to the Tabu River, covers an area of 150 ha. The study area presents typical steppe characteristics, with an average annual precipitation of 284 mm, an average annual ET of 2305 mm, and an annual average temperature of 2.5 °C. The zonal soil texture is Kastanozems. The type of land use and land cover

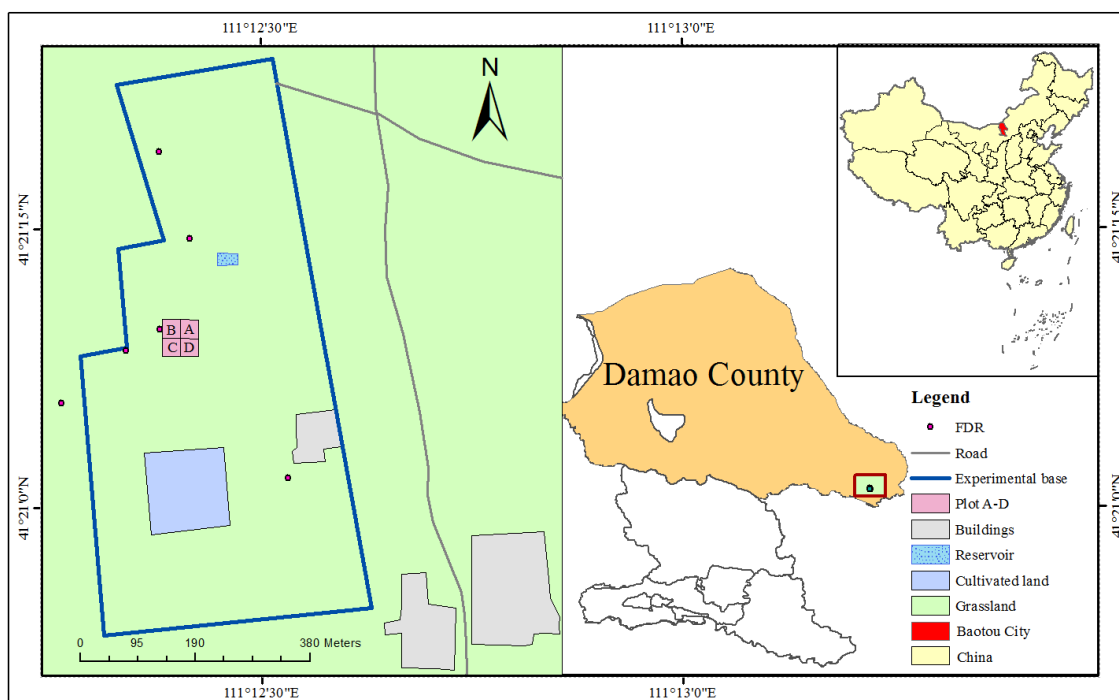(LULC) is uniform, and the grassland is mainly made up of *Leymus chinensis,* which is the dominant species.



**Figure 1.** The location of the study area.

## 3. Methodology

The methodology can be summarized as follows:

1.  According to the experiment design, GPR and the gravimetric method were both used to measure the soil moisture of four $30 \times 30$ m$^2$ plots.
2.  Based on the measuring results, a random combination method was applied to analyze the influence of a different number and sampling design of GPR survey lines on the measurement accuracy at pixel scale. Then, the necessary number and appropriate sampling design were obtained, resulting in a pixel-scale measurement method of soil moisture by GPR.
3.  The random combination method and the statistical sampling were used to determine the necessary sampling sizes of point measurements by gravimetric method under different accuracy requirements, respectively. Additionally, the pixel-scale measurement method by GPR and the sampling method by point measurements were compared.
4.  The soil moisture by remote sensing in the study area was retrieved by Landsat 8 data, obtaining the soil moisture of Plots A–D. The pixel-scale measurement method by GPR and the sampling method by point measurements were used to validate the remote sensing soil moisture in four plots, and the validation effects were analyzed, respectively.

### 3.1. GPR Theory

The transmitting antenna of GPR emits short pulses of electromagnetic waves into the soil. Part of the wave energy propagates towards the receiving antenna through the air; this is known as the airwave. Some of the wave energy transmits directly from the transmitting to receiving antenna in the soil along the air-ground interface; this is called the groundwave. When the radar wave encounters an interface or a target with a large electrical difference in the soil, part of the energy is reflected back to the ground and received by the receiving antenna. The receiving antenna records the propagation time, amplitude, waveform and other information of the returned wave in the soil, forming a radar recording profile. The

propagation velocity of the radar waves in the soil mainly depends on the soil dielectric permittivity, which in turn is strongly related to soil moisture [33]. To obtain the velocity, there are three commonly used methods, including the common-midpoint (CMP) method, the wide angle reflection and refraction (WARR) method, and the FO method. Both the CMP and WARR methods measure the radar wave velocity by increasing the distance between the transmitting antenna and the receiving antenna equidistantly (Figure 2). These two methods can quickly acquire the velocity of the ground wave and the reflected wave, but they are time consuming and have low spatial resolution [34]. However, the FO method provides higher spatial resolution and faster survey times than either the WARR or CMP method [35].
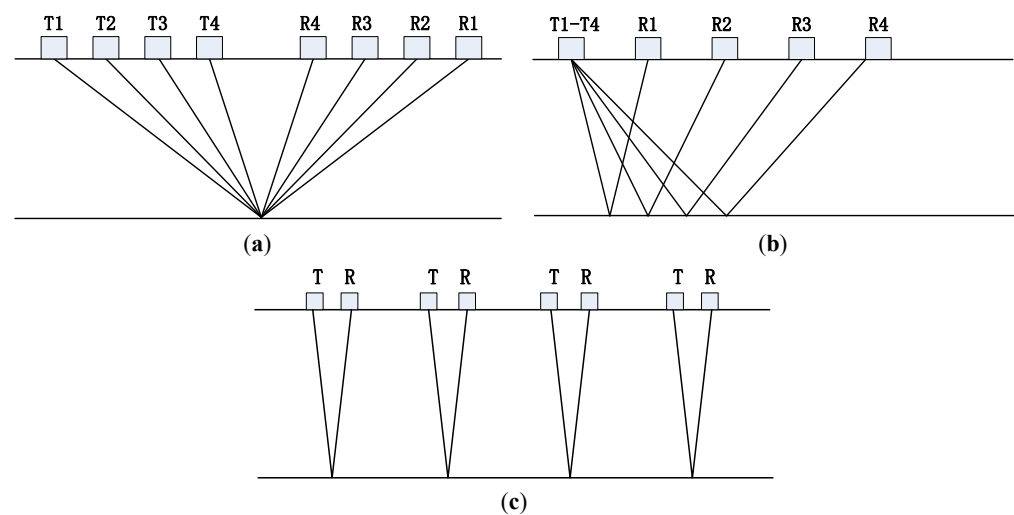


**Figure 2.** Schematic diagram of CMP method (**a**), WARR method (**b**) and FO method (**c**). ("T" means transmitting antenna, and "R" means receiving antenna. The bottom lines represent an interface or a target with a large electrical difference in the soil).

FO method is carried out by keeping the offset between the transmitter and receiver antenna fixed, and by moving antenna array along the survey line to measure the velocity of groundwave [35] (Figure 2). The velocity of groundwave is calculated from the arrival time of airwave ($t_{AW}$) and groundwave ($t_{GW}$), obtained by FO method at a known antenna separation ($x$ m):

$$v_{GW} = \frac{x}{(t_{GW} - t_{AW}) + \frac{x}{c}} \qquad (1)$$

In the soil, which is low-loss medium, ground wave velocity $v_{GW}$ can be converted to relative dielectric permittivity $\varepsilon$, using [36]

$$\varepsilon = (c/v_{GW})^2 \qquad (2)$$

where $c$ is the speed of the electromagnetic wave in free space.

Under natural conditions, soil moisture has the greatest influence on the measured dielectric permittivity of unsaturated soil [24]. For obtaining volumetric soil moisture $\theta$, an empirical relationship between $\varepsilon$ and $\theta$, proposed by Topp et al. (1980), is commonly used [33]:

$$\theta = -0.053 + 0.0293\varepsilon - 0.00055\varepsilon^2 + 0.0000043\varepsilon^3 \qquad (3)$$

The FO method can obtain the spatial distribution of soil moisture by extracting the ground wave, and does not require reflection layer depth. However, the accuracy of soil moisture measured by the FO method is affected by the time-zero calibration and the extraction of the ground wave travel time. Under dry conditions, the airwave and the ground wave interfere with each other when the antenna separation distance is too small; thus, the arrival time of the airwave and the ground wave cannot be accurately extracted.

When the antenna separation distance is too large under dry conditions, the ground wave is easily attenuated, and the spatial resolution is relatively low, which result in the inaccurate arrival time. Therefore, it is necessary to determine the optimum antenna separation distance by CMP or WARR before applying the FO method, so that $t_{GW}$ and $t_{AW}$ can be clearly distinguished and correctly identified. More specifically, the antenna separation distance was increased from 0.5 m to 3 m with an increment of 0.1 m using CMP method in this study, and then the minimum antenna separation distance can be found in the GPR profile; this resulted in an obvious difference between the arrival time of the transmitting antenna and the receiving antenna. Therefore, the antenna separation distance for the FO method was determined to be 1.5 m here.

The depth of soil moisture obtained by the FO method depends on the effective sampling depth of the ground wave. However, the sampling depth of ground waves is affected by various factors such as antenna frequency, soil moisture, soil texture, subsurface permittivity, etc. [37]. In this regard, researchers have carried out a number of relevant studies to estimate the sampling depth of ground wave [9,35,38,39]. Alternatively, Sperl (1999) suggested an empirical formula of sampling depth Z and radar wave length $\lambda$, which means that the sampling depth of ground wave by 250 MHz GPR is 0.1 m [39]:

$$Z \approx 0.145\lambda^{1/2} \tag{4}$$

### 3.2. Experiment Design

We selected $2 \times 2$ adjacent plots, each with an area of $30 \times 30$ m$^2$ (named Plot A, B, C, D in Figure 1), in flat terrain, as the experimental area. The soil moisture of four plots (Plots A, B, C, D) was measured by the FO method, and ten survey lines of GPR including four sides were arranged spaced 7.5 m apart in each plot which is divided into $4 \times 4$ units (Figure 3). In addition, there are two survey lines placed diagonally in each plot. In this study, the FO data were collected on 24 August 2016 using a PulseEKKOTM PRO GPR at a central frequency of 250 MHz, with an antenna separation of 1.5 m as determined by CMP method, a time window of 100 ns, a sampling interval of 0.4 ns and 32 stacks per trace. GPR moved along survey lines triggered every 0.1 m with an odometer, which resulted in at least 300 measurements per line. Meanwhile, gravimetric samples from 0.1 m depth were also collected every 7.5 m at 25 locations in each plot (Figure 3) for soil moisture measurement.
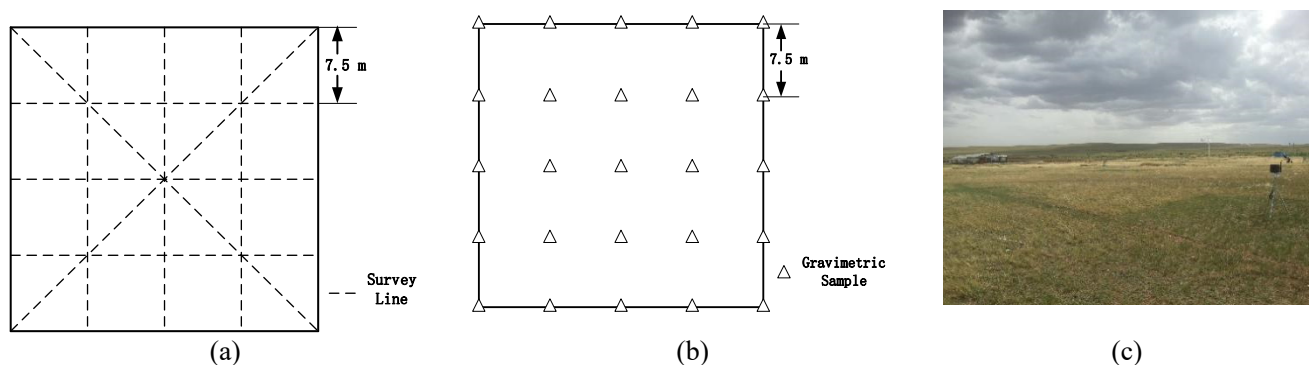


**Figure 3.** Experiment design of soil moisture measurement by GPR (**a**) and the gravimetric method (**b**). (the surrounding environment of the observation sites was shown in (**c**)).

### 3.3. Statistical Sampling

Statistical sampling is used to estimate the number of sampling points required to estimate the mean soil moisture with a specified confidence level and a given relative error [40]:

$$n = \frac{S^2 t_\alpha^2}{D^2} \tag{5}$$

where $S^2$ is the sample variance; $t_\alpha^2$ is the Student's t-statistic at the $\alpha$ probability level; and $D$ is the specified error limit.

### 3.4. Random Combination Method

The random combination method is an analysis method to estimate necessary sampling size proposed based on the bootstrap method, which can plot the relationship between the number of samples and the confidence level under different relative errors [17]. If there are n samples of soil moisture measurements in a pixel, $\theta_i$ (i = 1, 2, ... , n), the mean of the n samples can be used as the average soil moisture of the pixel when n is sufficiently large [17]. The method does not require any assumption of a sampling statistical distribution [17], but does not consider the spatial layout of the sampling points. It means that the GPR survey lines used in this method can be randomly positioned within the area. The basic steps for applying a random combination method to determine the sampling strategy are as follows:

1. Select *m* samples randomly from n samples (*m* = 1, 2, 3, ... , *n*), and repeat $C_n^m$ times to cover all the combinations each time.
2. Calculate the mean of *m* samples obtained by each selection, and obtain $C_n^m$ mean values in total.
3. Calculate the relative error between the $C_n^m$ mean and the mean of all *n* measured samples, and analyze the confidence level within 5%, 6%, 7%, 8%, 9%, and 10%.
4. Plot the relationship between the confidence level and *m* to determine the necessary sampling size corresponding to a given confidence level (95% or 90%) when the relative error ranges from 5% to 10%, respectively.

### 3.5. Remote Sensing Soil Moisture by Landsat 8

Under the same conditions, if soil water supply is sufficient, the plant grows well with strong evapotranspiration and relatively low land surface temperature. When vegetation is under drought stress, the lack of water at the root causes the leaf stomata to be closed, resulting in less evapotranspiration and increased land surface temperature. Then, the vegetation growth will be affected and the normalized difference vegetation index (NDVI) will decrease. Based on this principle, the vegetation supply water index (VSWI) was developed by Carlson et al. [41], which simply calculates a ratio between NDVI and surface temperature (LST), as follows:

$$\text{VSWI} = \frac{\text{NDVI}}{\text{LST}} \tag{6}$$

The greater the VSWI, the more vigorous the evapotranspiration of the vegetation, reflecting higher soil moisture. Otherwise, it means that the vegetation has insufficient water supply and the soil moisture is low.

Taking a total of seven cloudless Landsat 8 images from July to October in 2015 and in 2016 as data sources, the NDVI and the LST, estimated by a split-window algorithm which was developed by Du et al. (2015) and Ren et al. (2015), were used to calculate the VSWI of the study area [42,43]. By establishing a linear relationship between the VSWI and the soil moisture measurements at 0.05 m, the soil moisture by remote sensing was estimated from Landsat 8. The soil moisture measurements were obtained from six automatic monitoring instruments by frequency domain reflectometry (FDR) in the study area, as shown in Figure 1. Since there are no Landsat 8 data available on the day of the experiment, the Landsat 8 and MODIS data from two base times, which were before and after the experiment date, respectively (4 August 2015 and 5 September 2015), were blended by an enhanced spatial and temporal adaptive reflectance fusion model (ESTARFM) to predict Landsat 8 data on the day of the experiment. According to the relationship between VSWI and soil moisture, the corresponding soil moisture of the four plots from remote sensing on the day of the experiment can be calculated. In order to compare and analyze the soil moisture measurement results with GPR, the sampling depth of FDR was set at 0.1 m. Because the retrieval model for Landsat 8 soil moisture observations was trained by FDR data, the sensing depth of Landsat 8 is also 0.1 m.

## 4. Results

### 4.1. The Necessary Number of GPR Survey Lines for Pixel-Scale Soil Moisture

The FO method of GPR measures soil moisture in the form of survey lines. In this study, each survey line had about 300 soil moisture measurements at intervals of 0.1 m. The number of measuring points on single survey line far exceeded the necessary sampling size calculated by sampling methods based on point observations uniformly in any pixel. In order to further study the pixel-scale measurement method by GPR, this research applied the random combination method to analyze the necessary numbers of survey lines under different confidence levels and relative errors in four $30 \times 30 \text{ m}^2$ plots, as shown in Figure 4.
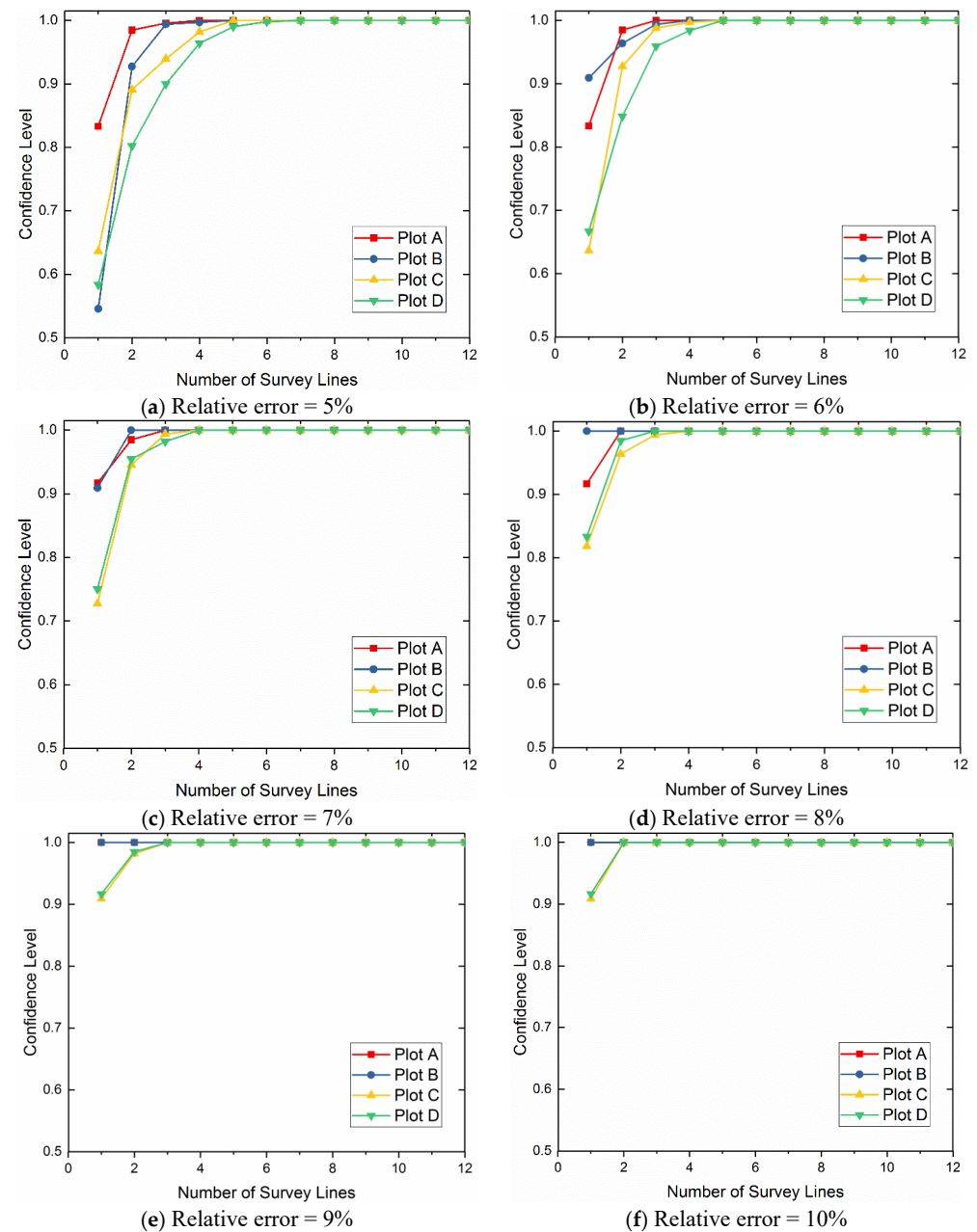


**Figure 4.** Relationship between the confidence level and number of survey lines under a given relative error ranging from 5% to 10% in Plot A, B, C and D.

In Figure 4, an increase in the number of survey lines resulted in a decrease in relative error under the same confidence level. This verified that the higher the required accuracy, the higher the number of survey lines needed. Under the relative error of 9% or 10%, one

survey line of GPR was enough to ensure that the confidence level was above 90% in any one of the four $30 \times 30$ m$^2$ plots. However, one survey line could no longer meet the ordinary accuracy requirement for a relative error of 7% or 8%. In any plot, two survey lines of GPR made the confidence level approach 95%, with a relative error of 7% or 8%. When the relative error was 5% or 6%, the confidence level corresponding to different numbers of survey lines changed more severely, and there were also significant differences in the results of different plots. The measurements by only 1 or 2 lines were highly variable and random. For example, the confidence level of one survey line in Plot B was only 55%. Under the relative error of 5% or 6% and a confidence level of 95%, the necessary number of survey lines for soil moisture was four in any one of the four $30 \times 30$ m$^2$ plots. Therefore, by arranging two survey lines in the pixel, the confidence level of the soil moisture measurements approached 95% for the relative error of 7%. The soil moisture results measured by four survey lines in the pixel had a confidence level greater than 95%, with a relative error of 5%.

The applicability of soil moisture measurements obtained by the above necessary number of survey lines was analyzed for the pixel with a resolution of 60 m. There were 24 survey lines laid evenly in a $60 \times 60$ m$^2$ plot area consisting of Plot A, B, C, D to measure soil moisture, and the random combination method was used to analyze the relationship between the number of survey lines and the confidence level under different relative errors (Figure 5). As shown in Figure 5, two survey lines of GPR would be sufficient to make the confidence level reach 95% with a relative error of 5%. Four survey lines of GPR can even ensure that soil moisture measurements had a confidence level of 100% under a relative error of 5%. The results showed that the necessary number of survey lines concluded from the pixel of 30 m resolution is equally applicable to the pixel with a resolution of 60 m.
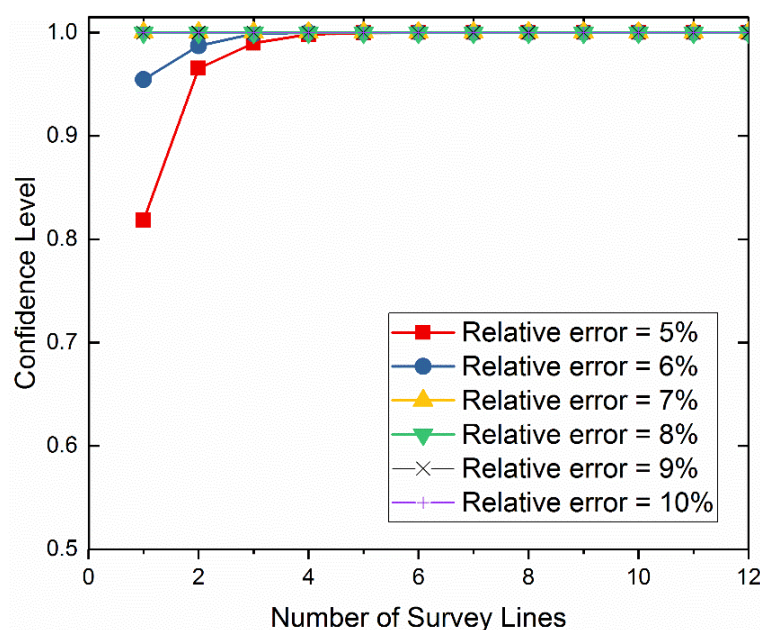


**Figure 5.** Relationship between the confidence level and number of survey lines under a given relative error ranging from 5% to 10% in a 60 m pixel.

### 4.2. The Sampling Design of GPR Survey Lines for Pixel-Scale Soil Moisture

It is often necessary to obtain the spatial distribution of soil moisture within the pixel while measuring the average soil moisture. According to the analysis of random sampling method, the number of survey lines used to measure soil moisture at pixel scale was determined, but different layouts of survey lines achieve different results in the spatial distribution map of soil moisture. In order to study the sampling design of survey lines, this research mapped the spatial distribution of soil moisture using universal kriging

interpolation in the four $30 \times 30$ m$^2$ plots [44]. The spatial distribution of soil moisture obtained from 12 survey lines in each plot was used as the reference, respectively, to analyze the influence of different layouts when measuring soil moisture by two or four survey lines, based on the necessary number of GPR survey lines for pixel scale; the results of Plot D were taken as an example, as shown in Figures 6 and 7.
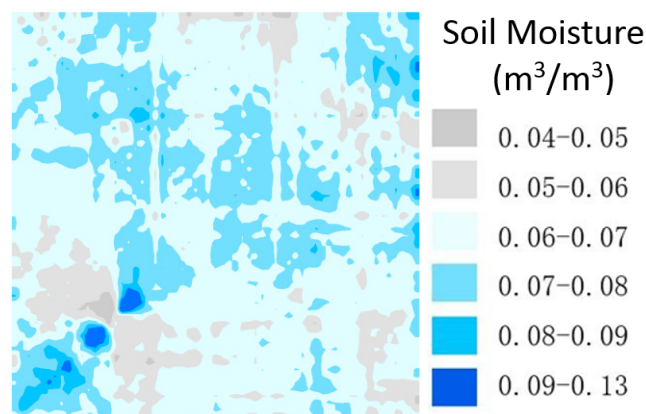


**Figure 6.** The location of the study area. Referenced spatial distribution map of soil moisture in Plot D.

When two lines are used to measure soil moisture in each plot, it is advisable to arrange survey lines to cover the plot evenly in order to better describe the spatial distribution. Considering this, the spatial distribution accuracy of soil moisture by two lines designed were compared in Shape I and Shape II (Table 1); this indicated that the results of these two layout methods were different. The spatial distribution accuracy of soil moisture in Plot B obtained by two lines in Shape I with an RMSE of 0.0076 m$^3$/m$^3$ was close to that in Shape II with an RMSE of 0.0079 m$^3$/m$^3$, which was similar to the accuracy of these two layout methods in Plot A and Plot C. For Plot D, the RMSE of Shape II was 0.0138 m$^3$/m$^3$, becoming significantly larger, because the estimation of soil moisture in the southwest was too high. However, the RMSE of Shape I was more stable, and the difference between the results of the four plots was small. It can be concluded that the two lines in Shape I were better with a smaller average RMSE of 0.0079 m$^3$/m$^3$. Therefore, on the premise of choosing two survey lines to measure pixel-scale soil moisture, the two lines designed in Shape I can accurately describe the spatial distribution of soil moisture with a relatively small estimation error.

**Table 1.** Spatial distribution accuracy of soil moisture measurements in different survey line shapes for Plot A–D.

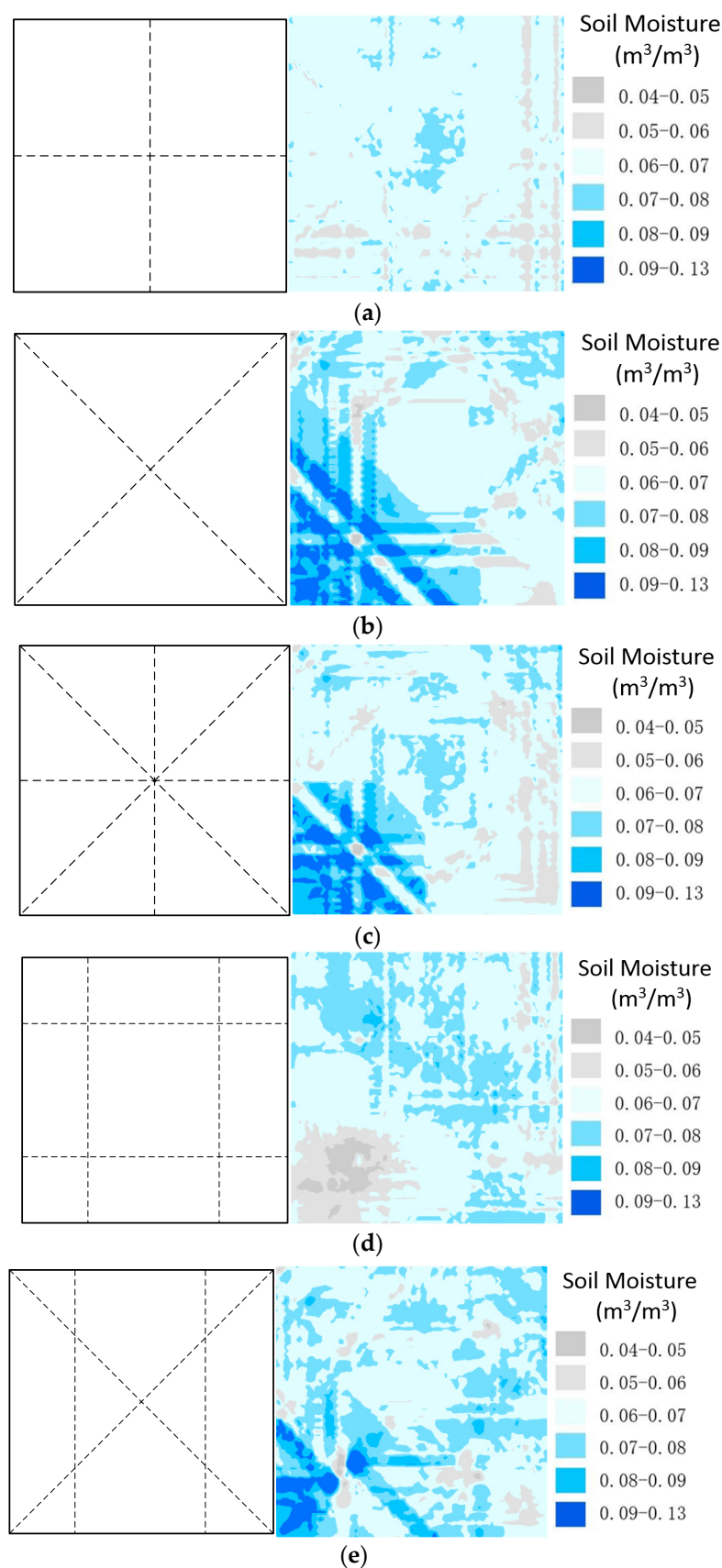| | RMSE (m$^3$/m$^3$) | | | | |
| --- | --- | --- | --- | --- | --- |
| | **Shape I** | **Shape II** | **Shape III** | **Shape IV** | **Shape V** |
| Plot A | 0.0083 | 0.0086 | 0.0066 | 0.0066 | 0.0067 |
| Plot B | 0.0076 | 0.0079 | 0.0063 | 0.0063 | 0.0065 |
| Plot C | 0.0078 | 0.0072 | 0.0059 | 0.007 | 0.0069 |
| Plot D | 0.0077 | 0.0138 | 0.0119 | 0.0087 | 0.0097 |
| Average | 0.0079 | 0.0094 | 0.0077 | 0.0072 | 0.0075 |

**Figure 7.** Spatial distributions of soil moisture in Plot D by two survey lines designed in Shape I (**a**) and Shape II (**b**), and by four survey lines in Shape III (**c**), Shape IV (**d**) and Shape V (**e**), respectively.

When using four survey lines to measure soil moisture, three uniform layout methods of Shape III, Shape IV, Shape V were analyzed by the spatial distribution maps of soil moisture (Table 1). For Plot D, the RMSE of soil moisture measurements by Shape III, Shape IV and Shape V were 0.0119 m$^3$/m$^3$, 0.0087 m$^3$/m$^3$ and 0.0097 m$^3$/m$^3$, respectively, reflecting that Shape IV had higher accuracy. Besides, the overall trend of soil moisture acquired by Shape IV was more similar to the referenced map than the other two layout methods. The results of Shape III and V overestimated the soil moisture of the southwest plot, so the RMSE tended to be larger. As shown in Table 1, the average RMSE of soil moisture measurements by Shape IV in all plots was 0.0072 m$^3$/m$^3$, which was the minimum among these three layout methods. Above all, the four lines designed in Shape IV were more appropriate for characterizing the spatial distribution of soil moisture in the pixel with small estimation error when four survey lines are used for pixel-scale soil moisture measurement.

The above conclusions were equally applicable to pixels with a resolution of 60 m, accurately mapping the spatial distribution of soil moisture.

*4.3. Pixel-Scale Measurement Method by GPR and Sampling Method by Point Measurements*

For the same plot, the necessary sampling sizes determined by different sampling methods of soil moisture based on point measurements under the same error were basically close (Table 2). For example, the necessary sampling sizes of Plot C, calculated by the statistical sampling and the random combination method, were 15 and 16, respectively, with a confidence level of 90% and a relative error of 5%. When the spatial variation of soil moisture is large, the sampling sizes calculated by different sampling methods using point measurements may produce greater difference, which makes it hard to determine the necessary sampling size and affect the ground validation of soil moisture obtained by remote sensing. On the other hand, the point-scale sampling methods usually require a large number of point measurements as a basis to analyze the necessary sampling size, and the preparatory work of data is time-consuming and labor-intensive. The demands of real-time data also make the point measurements difficult. Furthermore, the necessary sampling size based on point measurements is not universal, and may be quite different for another pixel because of the spatial heterogeneity of soil moisture. Even for the same pixel, it is essential to re-determine the necessary sampling size when monitoring soil moisture in different periods, which requires a lot of work and long time, due to its low measuring efficiency.

**Table 2.** The number of sampling points required under different accuracy by statistical sampling (referred as "S" in Table 2) and the random combination method (referred as "R" in Table 2).

| Confidence Level | Relative Error | Number of Sampling Points | | | | | | | |
|---|---|---|---|---|---|---|---|---|---|
| | | Plot A | | Plot B | | Plot C | | Plot D | |
| | | S | R | S | R | S | R | S | R |
| 90% | 5% | 16 | 16 | 11 | 10 | 15 | 16 | 15 | 15 |
| | 10% | 8 | 8 | 5 | 4 | 8 | 8 | 7 | 7 |
| 95% | 5% | 18 | 18 | 13 | 12 | 17 | 18 | 17 | 17 |
| | 10% | 10 | 10 | 6 | 5 | 10 | 9 | 10 | 9 |

The soil moisture measurements by GPR and point measurements are shown in Table 3. In Table 3, the two survey lines were arranged in Shape I, and the four survey lines were arranged in Shape IV. It was found that the soil moisture measurements of plots tended to be stable with the increase in the number of survey lines, and the stable value can be approximated as the true soil moisture of the pixel. The average soil moisture found by two survey lines in Shape I was equivalent to that found by 25 point measurements. The four survey lines in Shape IV can basically obtain stable and reliable observations of soil

moisture at pixel scale, and this result was more accurate than the measurements by 25 sampling points.

**Table 3.** Soil moisture measurements by gravimetric and GPR methods.

| Plot | Gravimetric Measurements (25 Samples/Plot) | Number of Survey Lines | | | | | |
|---|---|---|---|---|---|---|---|
| | | **1** | **2** | **4** | **8** | **10** | **12** |
| A | 0.069 | 0.064 | 0.071 | 0.071 | 0.070 | 0.070 | 0.071 |
| B | 0.058 | 0.055 | 0.060 | 0.063 | 0.060 | 0.061 | 0.061 |
| C | 0.066 | 0.061 | 0.070 | 0.069 | 0.068 | 0.067 | 0.068 |
| D | 0.071 | 0.060 | 0.066 | 0.066 | 0.065 | 0.066 | 0.065 |
| $60 \times 60$ m$^2$ | 0.064 (by 25 samples) 0.066 (by 81 samples) | 0.062 | 0.066 | 0.068 | 0.066 | 0.065 | 0.066 |

Under the same accuracy, the measurement method of soil moisture at pixel scale by GPR can better describe the spatial distribution of soil moisture in the pixel than the sampling methods using point measurements. For example, when the confidence level was 95% and the relative error was 5%, the spatial distributions of soil moisture in Plot C were mapped using universal kriging interpolation, according to the statistical sampling by point measurements and the pixel-scale measurement method by GPR, respectively (Figure 8). The measurement method of soil moisture at pixel scale by GPR has high spatial resolution with fast measurement.
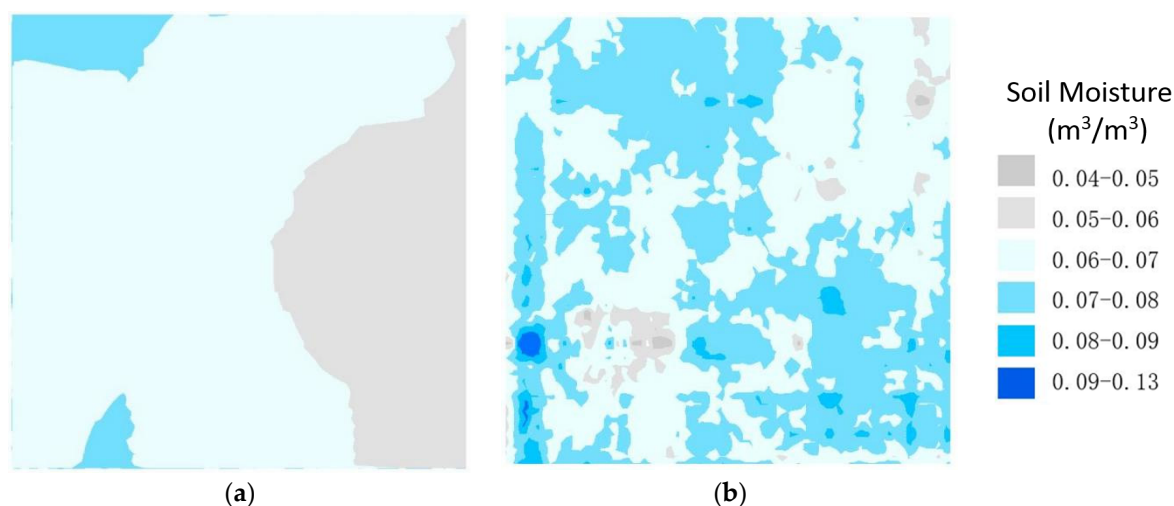


**Figure 8.** (**a**) Spatial distributions of soil moisture in Plot C by sampling method based on gravimetric data; (**b**) Spatial distributions of soil moisture in Plot C by pixel-scale measurement method based on GPR.

However, it should be noted that only the pixels with a resolution of 30 m and 60 m were analyzed in this study. Thus, the feasibility of the pixel-scale measurement method by GPR at other spatial scales needs further demonstration. In addition, the study area was located in the flat terrain of a desert steppe with single LULC. Thus the pixel-scale measurement method of soil moisture by GPR needs to be tested and improved under different LULC and in complex terrain. The measurement experiment of soil moisture also needs to be carried out in an area with high soil moisture values in order to verify the results of the analysis. The appropriate design of GPR survey lines may be different for pixels with large differences in soil moisture distribution. The survey line layout method in

this study is designed for pixels in which the spatial distribution difference in soil moisture is not particularly large.

### 4.4. Ground Validation Comparison of Remote Sensing Soil Moisture

The least square method was used to establish the linear model of soil moisture and VSWI calculated by Landsat 8 with $R^2$ of 0.71 and RMSE of 0.0216 m$^3$/m$^3$:

$$\theta = \text{VSWI} \times 8.581 - 0.049 \tag{7}$$

According to the above model, the soil moisture of the study area was obtained as shown in Figure 9. The remote sensing soil moisture of plots A–D were 0.037 m$^3$/m$^3$, 0.047 m$^3$/m$^3$, 0.043 m$^3$/m$^3$ and 0.046 m$^3$/m$^3$, respectively. The remote sensing results were both validated by point measurements and the pixel-scale measurements using GPR survey lines, as shown in Tables 4 and 5.
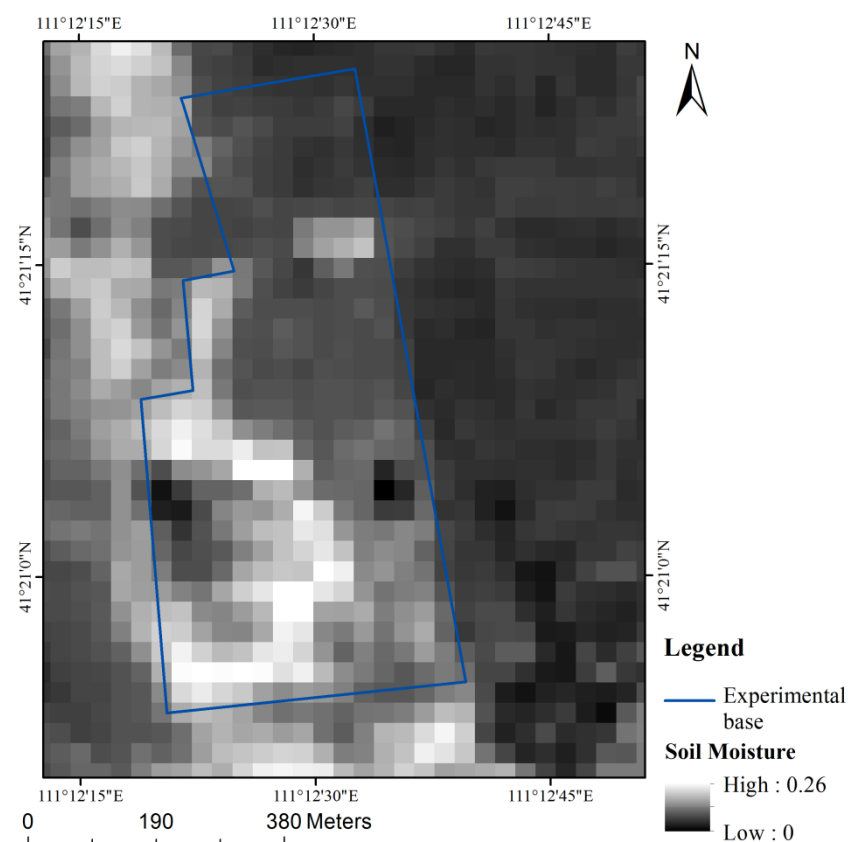


**Figure 9.** Spatial distribution of soil moisture in the study area obtained by Landsat 8.

**Table 4.** Ground validation of remote sensing soil moisture by point measurements.

| | Remote Sensing Soil Moisture (m$^3$/m$^3$) | Validation Results by Point Measurements (Relative Error) | | | | | |
|---|---|---|---|---|---|---|---|
| | | **1 Point** | **5 Points** | **10 Points** | **15 Points** | **20 Points** | **25 Points** |
| Plot A | 0.037 | 9.93–58.21% | 19.61–54.36% | 29.31–51.49% | 34.55–51.49% | 38.61–46.40% | 46.38% |
| Plot B | 0.047 | 3.90–37.10% | 2.62–29.08% | 6.74–26.16% | 10.91–23.69% | 14.27–20.78% | 18.97% |
| Plot C | 0.043 | 7.40–49.62% | 8.78–46.85% | 18.40–42.50% | 23.22–39.20% | 27.33–36.40% | 34.85% |
| Plot D | 0.046 | 11.20.–51.83% | 11.65–46.29% | 20.54–42.58% | 24.39–36.70% | 28.43–36.70% | 35.21% |
| | | 1 point | 5 points | 10 points | 15 points | 20 points | 25 points |
| RMSE of four plots (m$^3$/m$^3$) | | 0.0036–0.0438 | 0.0059–0.0365 | 0.0110–0.0316 | 0.0142–0.0284 | 0.0173–0.0250 | 0.0240 |

**Table 5.** Ground validation of remote sensing soil moisture by GPR survey lines.

| | Remote Sensing Soil Moisture (m³/m³) | Validation Results by GPR Survey Lines (Relative Error) | | | |
|---|---|---|---|---|---|
| | | **2 Lines** | **4 Lines** | **8 Lines** | **12 Lines** |
| Plot A | 0.037 | 47.60% | 47.89% | 47.14% | 47.89% |
| Plot B | 0.047 | 21.77% | 25.40% | 21.67% | 22.95% |
| Plot C | 0.043 | 38.71% | 37.68% | 36.76% | 36.76% |
| Plot D | 0.046 | 30.17% | 30.30% | 29.23% | 29.23% |
| | | 2 lines | 4 lines | 8 lines | 12 lines |
| RMSE of four plots (m³/m³) | | 0.0247 | 0.0249 | 0.0237 | 0.0242 |

Table 4 shows the validation results by point measurements of the gravimetric method. If any one of the 25 measuring points was used to validate the remote sensing results, the relative errors varied greatly, with a maximum difference of 48.27% for the same plot. The maximum difference between validation results by one point and 25 points was 36.44%. Moreover, the RMSE of four plots by one point was 0.0036 $m^3/m^3$ at the minimum and 0.0438 $m^3/m^3$ at the maximum. When the number of measuring points increased to any five of 25 measuring points, the difference in relative errors for the same plot became smaller but was still large, with a maximum difference of 38.06%. The range of RMSE was also smaller, with a difference of 0.0306 $m^3/m^3$. The maximum difference between validation results by any five points and 25 points was reduced to 26.77%. However, when the number of measuring points reached 20, the maximum difference of relative errors for the same plot was reduced to only 9.07%. The average RMSE of four plots varied from 0.0173 $m^3/m^3$ to 0.0250 $m^3/m^3$. In addition, the maximum difference between validation results by 20 points and 25 points was reduced to 7.77%. With the increase in point number, the variation range of validation results for the same plot decreased. However, the maximum difference of relative errors for the same plot did not decrease to less than 10% until it reached 20.

Table 5 shows the validation results using pixel-scale measurements of GPR survey lines, in which two lines and four lines were in Shape I and Shape IV, respectively, and eight lines were arranged without four sides. It can be clearly seen from the ground validation results that the relative errors and RMSE calculated by GPR with different line numbers were stable overall for the same plot. Compared with point measurements, the relative error extent is much smaller, with a maximum of only 3.73% under different line number. The average relative errors of four plots by two lines in Shape I and by four lines in Shape IV were 34.56% and 35.32%, respectively, which are less different than that by 25 measuring points. Just like the relative errors, the RMSE of soil moisture in four plots was stable, and in the range of 0.0237 $m^3/m^3$ and 0.0249 $m^3/m^3$. Additionally, the RMSE of four plots by two lines in Shape I and by four lines in Shape IV was 0.0247 $m^3/m^3$ and 0.0249 $m^3/m^3$, respectively, which was very close to that by 25 measuring points.

By comparing the validation results by two methods, it is obvious that the pixel-scale measurement method by GPR has obvious advantages in ground validation, with stable relative errors and less contingency, leading to more reliable ground validation results; this is more conducive to the accurate evaluation of remote sensing products. In this study, a pixel-scale measurement method of soil moisture by GPR has not been applied to the ground validation of quantitative products from remote sensing at other resolutions, except for 30 m resolution; these resolutions need further application.

## 5. Conclusions

With focus on the scale issue of soil moisture measurements for pixel, this research studied the pixel-scale measurement method by GPR, using a field experiment to provide a theoretical basis for validation and application of multi-scale soil moisture products by remote sensing. According to the soil moisture measurements in $30 \times 30$ m$^2$ plots, the sampling method of point measurements and the number and different layouts of GPR survey lines were analyzed by a random combination method and universal kriging interpolation to propose a pixel-scale measurement method of soil moisture based on GPR. Two survey lines of GPR would be sufficient under a confidence level of 90% and a relative error of 7%, and four survey lines of GPR would be eligible with a confidence level of 95% and a relative error of 5% for the pixel with a resolution of 30 m. Compared to other sampling methods by point measurements, the GPR measurement can produce the spatial distribution of soil moisture with higher resolution and smaller estimation errors, especially when two and four survey lines are designed in a cross shape (Shape I) and grid shape (Shape IV), respectively. The stable and reliable measurements by four survey lines in grid shape is closer to the true soil moisture of pixel than the sampling method by point measurements. Additionally, the applicability of the above conclusion to the pixel with a resolution of 60 m has been verified. In addition, the pixel-scale measurement method of soil moisture based on GPR was applied to ground validation for the soil moisture results monitored by Landsat 8, showing that the average relative errors and RMSE by two lines in Shape I were 34.56% and 0.0247 m$^3$/m$^3$, and those by four lines in Shape IV were 35.32% and 0.0249 m$^3$/m$^3$, respectively. The validation results suggested that the pixel-scale measurement method of soil moisture using GPR has more advantages than the traditional method of point measurement in ground validation, with stable relative errors and less contingency leading to more reliable evaluation in remote sensing products. The proposed method does not require a large amount of sampling data as the basis for analysis, thereby saving on measurement costs and improving measurement efficiency. Moreover, GPR is highly efficient and easy to move, and can repeatedly measure soil moisture in the same place. The pixel-scale measurement method of soil moisture by GPR bridges the scale gap between remote sensing and point measurement to reduce errors in ground validation for remote sensing results; it is a fast and reasonable way to estimate a rational mean value of pixel-scale soil moisture.

## Abbreviations

| | |
|---|---|
| GPR | Ground-penetrating radar |
| FO | Fixed offset |
| ET | Evapotranspiration |
| TDR | Time domain reflectometry |
| LULC | Land use and land cover |
| CMP | Common-midpoint |
| WARR | Wide angle reflection and refraction |
| NDVI | Normalized difference vegetation index |
| LST | Land surface temperature |
| VSWI | Vegetation supply water index |
| FDR | Frequency domain reflectometry |
| ESTARFM | Enhanced spatial and temporal adaptive reflectance fusion model |

## References

1.  Pal, M.; Maity, R. Development of a spatially-varying statistical soil moisture profile model by coupling memory and forcing using hydrologic soil groups. *J. Hydrol.* **2019**, *570*, 141–155. [CrossRef]
2.  Park, S.; Im, J.; Park, S.; Rhee, J. Drought monitoring using high resolution soil moisture through multi-sensor satellite data fusion over the Korean peninsula. *Agric. For. Meteorol.* **2017**, *237–238*, 257–269. [CrossRef]
3.  Champagne, C.; Mcnairn, H.; Berg, A.A. Monitoring agricultural soil moisture extremes in Canada using passive microwave remote sensing. *Remote Sens. Environ.* **2011**, *115*, 2434–2444. [CrossRef]
4.  Maity, R.; Sharma, A.; Nagesh Kumar, D.; Chanda, D. Characterizing drought using the reliability-resilience-vulnerability concept, special issue on Data Driven Approaches to Droughts. *J. Hydrol. Eng. ASCE* **2013**, *18*, 859–869. [CrossRef]
5.  Padhee, S.K.; Nikam, B.R.; Dutta, S.; Aggarwal, S.P. Using satellite-based soil moisture to detect and monitor spatiotemporal traces of agricultural drought over Bundelkhand region of India. *GISci. Remote Sens.* **2017**, *54*, 144–166. [CrossRef]
6.  Engman, E.T. Applications of microwave remote sensing of soil moisture for water resources and agriculture. *Remote Sens. Environ.* **1991**, *35*, 213–226. [CrossRef]
7.  Keshavarz, M.R.; Vazifedoust, M.; Alizadeh, A. Drought monitoring using a soil wetness deficit index (SWDI) derived from MODIS satellite data. *Agric. Water Manag.* **2014**, *132*, 37–45. [CrossRef]
8.  Thiruvengadam, P.; Rao, Y.S. Spatio-temporal variation of soil moisture and drought monitoring using passive microwave remote sensing. In Proceedings of the 2016 IEEE International Geoscience and Remote Sensing Symposium, Beijing, China, 10–15 July 2016; IEEE: Piscataway, NJ, USA, 2016. [CrossRef]
9.  Van Overmeeren, R.A.; Sariowan, S.V.; Gehrels, J.C. Ground penetrating radar for determining volumetric soil water content; results of comparative measurements at two test sites. *J. Hydrol.* **1997**, *197*, 316–338. [CrossRef]
10. Bolten, J.D.; Crow, W.T.; Zhan, X.; Jackson, T.J.; Reynolds, C.A. Evaluating the utility of remotely sensed soil moisture retrievals for operational agricultural drought monitoring. *IEEE J. Sel. Top. Appl. Earth Obs. Remote Sens.* **2010**, *3*, 57–66. [CrossRef]
11. Pal, M.; Maity, R.; Suman, M.; Das, S.K.; Patel, P.; Srivastava, H.S. Satellite based Probabilistic Assessment of Soil Moisture using C-band Quad-polarized RISAT 1 data. *IEEE Trans. Geosci. Remote Sens.* **2017**, *55*, 1351–1362. [CrossRef]
12. Lu, Y.; Song, W.; Lu, J.; Su, Z.; Liu, H.; Tan, Y.; Han, J. Soil water measurement by ground penetrating radar and its scale features, South-to-North Water Diversion Project. *Water Sci. Technol.* **2017**, *15*, 37–44. [CrossRef]
13. Yu, W.; Zhang, Y.; Chen, L.; Zheng, S. Soil moisture estimation based on TVDI and meteorological factors. *Geospat. Inf.* **2015**, *13*, 137–139.
14. Gilbert, R.O. *Statistical Methods for Environmental Pollution Monitoring*; Van Nostrand Reinhold Company, Inc.: New York, NY, USA, 1987; pp. 26–54. [CrossRef]
15. Kamgar, A.; Hopmans, J.W.; Wallender, W.W.; Wendroth, O. Plot size and sample number for neutron probe measurements in small field trials. *Soil Sci.* **1993**, *156*, 213–224. [CrossRef]
16. Sastre, J.; Vidal, M.; Rauret, G.; Sauras, T. A soil sampling strategy for mapping trace element concentrations in a test area. *Sci. Total Environ.* **2010**, *264*, 141–152. [CrossRef] [PubMed]
17. Wang, C.; Zuo, Q.; Zhang, R. Estimating the necessary sampling size of surface soil moisture at different scales using a random combination method. *J. Hydrol.* **2008**, *352*, 309–321. [CrossRef]
18. Zhang, R. *Applied Geostatistics in Environmental Science*; Science Press USA Inc.: Monmouth Junction, NJ, USA, 2005; pp. 91–92.
19. Huisman, J.A.; Snepvangers, J.J.J.C.; Bouten, W.; Heuvelink, G.B.M. Mapping spatial variation in surface soil water content: Comparison of ground-penetrating radar and time domain reflectometry. *J. Hydrol.* **2002**, *269*, 194–207. [CrossRef]
20. Huisman, J.A.; Sperl, C.; Bouten, W.; Verstraten, J.M. Soil water content measurements at different scales: Accuracy of time domain reflectometry and ground-penetrating radar. *J. Hydrol.* **2001**, *254*, 48–58. [CrossRef]
21. Illawathure, C.; Parkin, G.; Lambot, S.; Galagedara, L. Evaluating soil moisture estimation from ground-penetrating radar hyperbola fitting with respect to a systematic time-domain reflectometry data collection in a boreal podzolic agricultural field. *Hydrol. Process.* **2020**, *34*, 1428–1445. [CrossRef]

22. Klotzsche, A.; Jonard, F.; Looms, M.C.; van der Kruk, J.; Huisman, J.A. Measuring soil water content with ground penetrating radar: A decade of progress. *Vadose Zone J.* **2018**, *17*, 180052. [CrossRef]

23. Galagedara, L.W.; Parkin, G.W.; Redman, J.D.; von Bertoldi, P.; Endres, A.L. Field studies of the GPR ground wave method for estimating soil water content during irrigation and drainage. *J. Hydrol.* **2005**, *245*, 182–197. [CrossRef]

24. Hubbard, S.; Grote, K.; Rubin, Y. Mapping the volumetric soil water content of a California vineyard using high-frequency GPR ground wave data. *Lead. Edge* **2002**, *21*, 552–559. [CrossRef]

25. Grote, K.; Hubbard, S.; Rubin, Y. Field-scale estimation of volumetric water content using ground-penetrating radar ground wave techniques. *Water Resour. Res.* **2003**, *39*, 1321–1335. [CrossRef]

26. Lunt, I.A.; Hubbard, S.S.; Rubin, Y. Soil moisture content estimation using ground-penetrating radar reflection data. *J. Hydrol.* **2005**, *307*, 254–269. [CrossRef]

27. Steelman, C.M.; Endres, A.L.; Jones, J.P. High-resolution ground-penetrating radar monitoring of soil moisture dynamics: Field results, interpretation, and comparison with unsaturated flow model. *Water Resour. Res.* **2012**, *48*, W09538. [CrossRef]

28. Liu, X.; Cui, X.; Guo, L.; Chen, J.; Li, W.; Yang, D.; Cao, X.; Chen, X.; Liu, Q.; Lin, H. Non-invasive estimation of root zone soil moisture from coarse root reflections in ground-penetrating radar images. *Plant Soil* **2019**, *436*, 623–639. [CrossRef]

29. Minet, J.; Bogaert, P.; Vanclooster, M.; Lambot, S. Validation of ground penetrating radar full-waveform inversion for field scale soil moisture mapping. *J. Hydrol.* **2012**, *424–425*, 112–123. [CrossRef]

30. Qin, Y.; Chen, X.; Zhou, K.; Klenk, P.; Roth, K.; Sun, L. Ground-penetrating radar for monitoring the distribution of near-surface soil water content in the Gurbantunggut Desert. *Environ. Earth Sci.* **2013**, *70*, 2883–2893. [CrossRef]

31. Weihermüller, L.; Huisman, J.A.; Lambot, S.; Herbst, M.; Vereecken, H. Mapping the spatial variation of soil water content at the field scale with different ground penetrating radar techniques. *J. Hydrol.* **2007**, *340*, 205–216. [CrossRef]

32. Lu, Y.; Song, W.; Lu, J.; Wang, X.; Tan, Y. An Examination of Soil Moisture Estimation Using Ground Penetrating Radar in Desert Steppe. *Water* **2017**, *9*, 521. [CrossRef]

33. Topp, G.C.; Davis, J.L.; Annan, A.P. Electromagnetic determination of soil water content: Measurements in coaxial transmission lines. *Water Resour. Res.* **1980**, *16*, 574–582. [CrossRef]

34. Liu, Y.; James, I.; Klaus, H. High-resolution velocity estimation from surface-based common-offset GPR reflection data. *Geophys. J. Int.* **2022**, *230*, 131–144. [CrossRef]

35. Galagedara, L.W.; Redman, J.D.; Parkin, G.W.; Annan, A.P.; Endres, A.L. Numerical modeling of GPR to determine the direct ground wave sampling depth. *Vadose Zone J.* **2005**, *4*, 1096–1106. [CrossRef]

36. Davis, J.L.; Annan, A.P. Ground penetrating radar for high resolution mapping of soil and rock stratigraphy. *Geophys. Prospect.* **1989**, *37*, 531–551. [CrossRef]

37. Steelman, C.M.; Endres, A.L. An examination of direct ground wave soil moisture monitoring over an annual cycle of soil conditions. *Water Resour. Res.* **2010**, *46*, W11533. [CrossRef]

38. Du, S. *Determination of Water Content in the Subsurface with the Ground Wave of Ground Penetrating Radar*; Ludwig-Maximilians-Universitat: München, Germany, 1996.

39. Sperl, C. Erfassung der Raum-Zeitlichen Variation des Boden-Wassergehaltes in Einem Agrarokosystem mit dem Ground-Penetrating Radar. Ph.D. Thesis, Technische Universitat, München, Germany, 1999; p. 182.

40. Petersen, R.G.; Calvin, L.D. Sampling. In *Methods of Soil Analysis. Part 1. Physical and Mineralogical Methods. Agronomy Monographs No. 9*, 2nd ed.; Klute, C.A., Ed.; American Society of Agronomy Inc.: Madison, WI, USA, 1986; pp. 33–51.

41. Carlson, T.N.; Gillies, R.R.; Perry, E.M. A method to make use of thermal infrared temperature and NDVI measurements to infer surf ace soil water content and fractional vegetation cover. *Remote Sens. Rev.* **1994**, *9*, 161–173. [CrossRef]

42. Du, C.; Ren, H.; Qin, Q.; Meng, J.; Zhao, S. A practical split-window algorithm for estimating land surface temperature from Landsat 8 data. *Remote Sens.* **2015**, *7*, 647–665. [CrossRef]

43. Ren, H.; Du, C.; Liu, R.; Qin, Q.; Yan, G.; Li, Z.; Meng, J. Atmospheric water vapor retrieval from Landsat 8 thermal infrared images. *J. Geophys. Res. Atmos.* **2015**, *120*, 1723–1738. [CrossRef]

44. Li, H.; Lin, Z.; Liu, S. Application of Kriging Technique in estimating soil moisture in China. *Geogr. Res.* **2001**, *20*, 446–452. [CrossRef]